Theoretical Studies on Isoprene Ozonolysis under Tropospheric Conditions. 1. Reaction of Substituted Carbonyl Oxides with Water

P. Aplincourt[†,‡] and J. M. Anglada*[,†]

Departament de Química Orgànica Biològica, Institut d'Investigacions Químiques i Ambientals de Barcelona, IIQAB-CSIC, c/ Jordi Girona 18, E-08034 Barcelona, Catalunya, Spain, and Laboratoire de Chimie Théorique et Matériaux Hybrides, Ecole Normale Supérieure de Lyon, 46 allée d'Italie, 69364 Lyon, Cedex 07, France

Received: August 29, 2002; In Final Form: April 30, 2003

The reactions between isoprene carbonyl oxides and water have been investigated using density functional theory and large scale ab initio methods. These reactions begin with the formation of a hydrogen-bond complex and may follow two different reaction paths. The main one corresponds to the water addition to carbonyl oxide and leads to the formation of α-hydroxy hydroperoxides. This process is exothermic by about 38 kcal mol^{-1} and, depending on the particular carbonyl oxide, has activation enthalpies in the 9−15 kcal mol^{-1} range with respect to the corresponding H-bond complex. For carbonyl oxides having *β*-hydrogen substitutes in syn configuration with respect to the COO unit, a hydrogen-transfer reaction path leading to the formation of OH radicals is also possible. In this case the branching ratio has been calculated at different temperatures. This ratio is computed to be 13.5% at 298.14 K but rises up to 20.4% at 273 K because of a strong tunneling effect.

Introduction

Nonmethane hydrocarbons (NMHC) are emitted to the atmosphere from both biogenic and anthropogenic origin and play a major role in ozone formation in rural and urban areas.[1,2] Their oxidation into peroxyl radicals triggers ozone production, thanks to the conversion of NO into NO_2. NMHC are also a source of organic acids, which can contribute to regional acid deposition.[3] Isoprene (2-methylbuta-1,3 diene, $CH_2{=}CH(CH_3)C{=}CH_2$) is one of the most important NMHC in the atmosphere. It is emitted to the troposphere in large amounts, up to 503×10^9 kg/yr[4] and has a lifetime from tens of minutes to a few hours.[5,6] The most important source of isoprene has a biogenic origin, since this compound is emitted from vegetation.[7,8] Lamb et al. have shown that isoprene represents about 80% of the hydrocarbons emitted by deciduous forests.[9] The biogenic emission is driven by photosynthesis and is therefore a maximum during summer time, when temperature and solar radiation are the highest.[10] The other source of isoprene is anthropogenic and comes from motor vehicles principally. This source reaches its maximum in winter as a consequence of cold starts.[11] Atmospheric oxidation of isoprene is initiated by reaction with OH, NO_3, or O_3,[12] which often lead to the production of oxygenated and nitrated intermediates. The gas-phase reaction of ozone with isoprene is an important oxidation process in the troposphere. It takes place during day and night and is linked to several important atmospheric species. There is convincing experimental evidence that alkene ozonolysis constitutes an important source of OH radicals. These radicals are the dominant sink for methane, carbon monoxide, and many other organic substances in the atmosphere and are therefore often called the "detergent of the atmosphere". Ozonolysis may even compete with the photolysis of O_3 in the daytime and with reactions initiated by NO_3 at night.[13−27,79] Quantum mechanical calculations have also clarified and confirmed the mechanism leading to OH formation.[28−33] Under atmospheric conditions, the alkene ozone reaction also produces H_2O_2. This other important oxidant damages trees and plants and contributes to the acid rain by the conversion of SO_2 into H_2SO_4.[34−36] In addition, organic acids and aldehydes are also directly produced during the ozonolysis of alkenes. Consequently, the atmospheric importance of isoprene ozonolysis is very high.

Regarding the reaction mechanism, O_3 adds initially to both double bonds of isoprene, yielding the 1,2 and 3,4 primary ozonides (eq 1a) in the so-called Criegee mechanism.[37] These

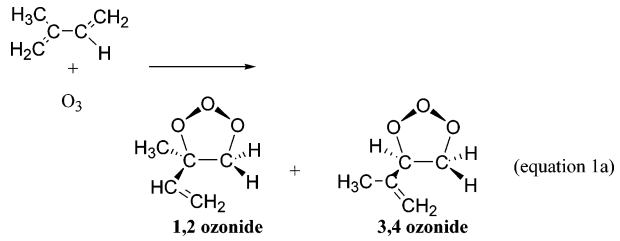

(equation 1a)

two ozonides are formed with an excess of vibrational energy and decompose into nine different carbonyl oxides (Criegee intermediates) and three carbonyl compounds [formaldehyde, methyl vinyl ketone (**MVK**), and methacroleine (**MAC**)] (see eqs 1b and 1c). In addition, it must be noted that two other decomposition pathways for primary ozonides are possible. They begin with the cleavage of the O−O bond in the primary ozonides and produce OH radicals via an unstable hydroperoxide intermediate.[38,39]

The nine carbonyl oxides (H_2COO and those labeled **M1a** to **M1h**) are formed with an excess of vibrational energy and may undergo unimolecular decomposition. Nevertheless, an important fraction of them are vibrationally stabilized and further

* Corresponding author. E-mail: anglada@iiqab.csic.es.
† Institut d'Investigacions Químiques i Ambientals de Barcelona.
‡ Ecole Normale Supérieure de Lyon.

10.1021/jp026868o CCC: $25.00
Published on Web 07/08/2003

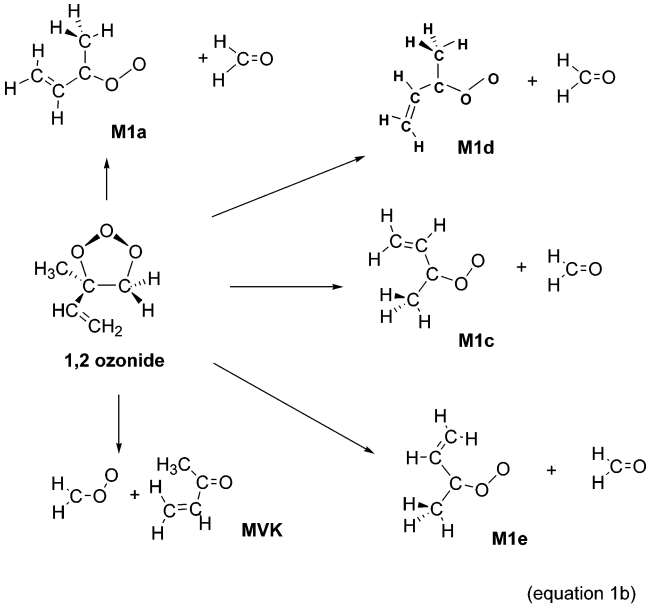

(equation 1b)

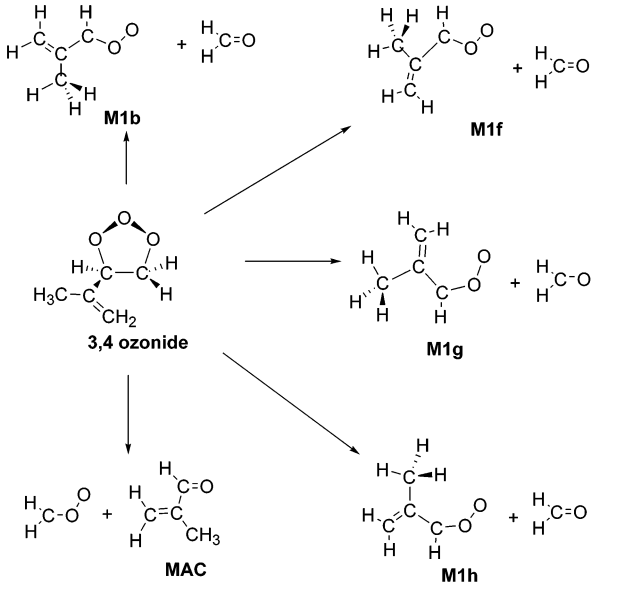

(equation 1c)

react with other atmospheric species.[40,41] The unimolecular decomposition has been recently investigated [30,38,39] and constitutes an important source of OH radicals. Other products such as CO or CO_2 are also obtained via the isomerization into the corresponding dioxirane intermediate. The corresponding reaction mechanisms (hydroperoxide and ester channel respectively) are well-known and have been investigated for the isoprene carbonyl oxides and for other carbonyl oxides.[42−49]

With respect to the bimolecular reactions, the reaction with water vapor is one of the most important processes for the atmospheric degradation of the stabilized carbonyl oxides.[50,51] It is known that this reaction leads to the formation of α-hydroxy hydroperoxide compounds, organic acids, aldehydes, and H_2O_2.[55,74−78] These species have been detected in air and precipitation, in forested and urban areas under atmospheric polluted conditions.[52−58] The environmental importance of this reaction is therefore clear and an accurate knowledge of the mechanism and products formed is necessary.

Previous theoretical studies on the reaction of water with the parent H_2COO as well as the methyl- and dimethyl-substituted carbonyl oxides have indicated that this reaction follows the three-step mechanism depicted in eq 2.[59−61] After the formation

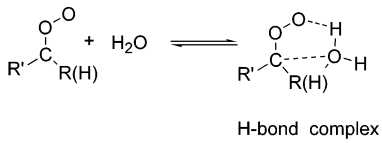

(equation 2a)

H-bond complex

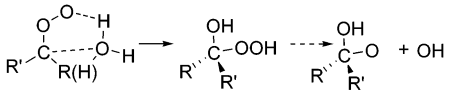

(equation 2b)

H-bond complex

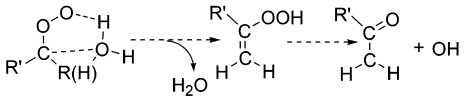

(equation 2c)

H-bond complex

of an hydrogen-bond complex, two reaction pathways are possible. First, a α-hydroxy hydroperoxide can be formed by the addition of the water molecule to the carbonyl oxide (eq 2b). Second, a transfer of a hydrogen atom belonging to the carbonyl oxide to the terminal oxygen of the COO group can take place with the help of the water molecule (eq 2c). The hydroperoxide intermediate then leads to the OH radical by OO bond breaking. This process corresponds to the water-catalyzed reaction of the hydroperoxide channel described in the case of the unimolecular decomposition of carbonyl oxides.[30,38,39]

Following those theoretical studies, the reaction of water with all the eight isoprene carbonyl oxides (**M1a**−**M1h**; see eq 1) has been investigated in the present paper. High-level theoretical calculations have been performed in order to clarify the reaction mechanism and to bring light to the important questions of atmospheric interest concerning the possible formation of OH radicals via this mechanism. In the next paper[83] we will also report a theoretical study on the unimolecular and water-assisted decomposition of the α-hydroxy hydroperoxides formed during the reaction between water and the **M1a**−**M1h** carbonyl oxides.

Computational Details

Geometry optimization of all the species considered in this study have been first carried out in DFT at the B3LYP/6-31G(d,p) level of theory.[62,63] At this level, harmonic vibrational frequencies have been calculated to verify the nature of the corresponding stationary point (minima or transition state) as well as to provide the zero point vibrational energy (ZPE) and the thermodynamic contributions to the enthalpy and the free energy. Moreover, to ensure that the transition states connect the desired reactants and products, intrinsic reaction coordinate calculations (IRC) have been performed for each transition state of every elementary reaction.

In a second step, all stationary points have been reoptimized using the B3LYP approach with the more flexible 6-311+G(2d,2p) basis set, [64] which allows a better description of hydrogen-bond complexes and transition structures involving hydrogen transfer considered in this work. At this level of theory, basis set superposition errors (BSSE) have been corrected for all the hydrogen-bond complexes by the counterpoise method of Boys and Bernardi.[65]

In a third step, high-level single-point energy G2 (G2M-RCC5)[66] calculations have been performed on the

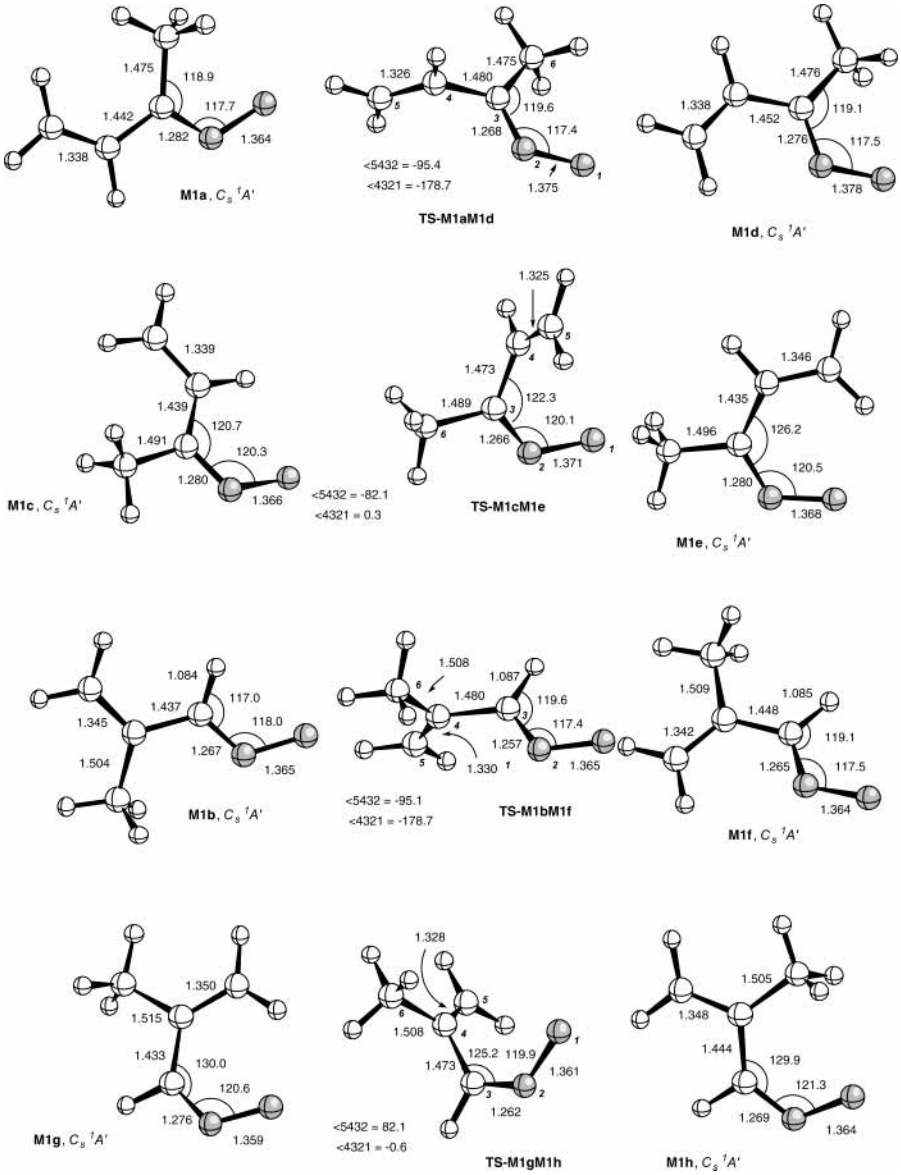

Figure 1. Selected B3LYP/6-311+G(2d,2p) geometrical parameters of the isoprene carbonyl oxides and the transition structures connecting the cis and trans isomers.

TABLE 1: Zero Point Energies (ZPE in kcal mol^{-1}), Entropies (*S* in eu) and Relative Energies, Enthalpies and Free Energies (*E*, *H*, and *G* in kcal mol^{-1}) for the Carbonyl Oxides M1a, M1b, M1c, M1d, M1e, M1f, M1g, and M1h and the Transition States Connecting These Structures

				B3LYP/6-311+G(2d,2p)			G2M-RCC5			CCSD(T)/6311+G(2df,2p)		
compound	ZPE[a]	S^a	relative to	E	E + ZPE	H_{298}	E	E + ZPE	H_{298}	E	E + ZPE	H_{298}
M1a	58.5	78.8		0.0	0.0	0.0	0.0	0.0	0.0	0.0	0.0	0.0
TS-M1aM1d	57.8	76.8	**M1a**	9.3	8.6	8.3	8.2	7.6	7.3			
M1d	58.4	79.6	**M1a**	2.0	1.9	1.9	1.8	1.6	1.7	1.8	1.7	1.8
M1b	58.6	79.3	**M1a**	5.7	5.7	5.8	5.5	5.6	5.6	5.8	5.9	5.9
TS-M1bM1f	58.0	77.2	**M1b**	10.9	10.3	9.9	9.5	8.9	8.6			
M1f	58.4	80.6	**M1a**	9.5	9.4	9.5	8.8	8.6	8.8	9.2	9.1	9.2
M1c	58.5	79.6	**M1a**	2.7	2.6	2.7	2.7	2.7	2.8	2.8	2.7	2.8
TS-M1cM1e	57.8	77.5	**M1c**	9.7	9.0	8.8	8.7	8.0	7.7			
M1e	58.5	79.0	**M1a**	2.7	2.7	2.7	2.6	2.6	2.7	2.8	2.8	2.8
M1g	58.7	79.0	**M1a**	7.3	7.5	7.5	6.3	6.5	6.4	6.6	6.8	6.8
TS-M1gM1h	58.1	76.2	**M1g**	9.3	8.8	8.4	8.3	7.7	7.4			
M1h	58.8	79.0	**M1a**	8.7	9.0	8.9	8.1	8.4	8.3	8.1	8.4	8.4

[a] The ZPE and *S* values have been computed at the B3LYP/6-31G(d,p) level of theory.

B3LYP/6-311+G(2d,2p) geometries of all the stationary points in order to obtain more reliable energy values. The G2 (G2M-RCC5) model suggested by Mebel et al. requires RCCSD(T)/6-311G(d,p),[67] RMP2/6-311G(d,p),[68] and RMP2/6-311+G(3df,2p) single point calculations and includes "high level corrections" (HLC) based on the number of paired and unpaired electrons and zero point energy (ZPE) corrections. The G2M-RCC5 model has been applied to compute atomization

TABLE 2: Zero Point Energies (ZPE in kcal mol^{-1}), Entropies (*S* in eu), and Reaction and Activation Energies, Enthalpies, and Free Energies (*E*, *H*, and *G* in kcal mol^{-1}) for the reaction between M1a, M1d, M1c, and M1e with H_2O

compound	ZPE[a]	S[a]	relative to	method	ΔE(ZPE)[b]	ΔH_{298}[b]	ΔG_{298}[b]
M1a + H_2O	71.9	124.0		B3LYP	0.0	0.0	0.0
				G2M-RCC5	0.0	0.0	0.0
				CCSD(T)	0.0	0.0	0.0
M2a	74.1	94.9	**M1a** + H_2O	B3LYP	−5.9 (−5.5)	−6.4 (−6.0)	2.3 (2.7)
				G2M-RCC5	−6.1 (−5.7)	−6.6 (−6.2)	2.1 (2.5)
				CCSD(T)	−7.0 (−6.6)	−7.5 (−7.1)	1.1 (1.5)
TS-M2aM3a	73.1	84.4	**M2a**	B3LYP	17.0	15.9	19.0
				G2M-RCC5	15.9	14.8	17.9
				CCSD(T)	15.5	14.4	17.5
M3a	75.8	85.6	**TS-M2aM3a**	B3LYP	−31.3	−31.1	−31.4
				G2M-RCC5	−38.5	−38.2	−38.6
				CCSD(T)	−38.6	−38.3	−38.7
R2a + **OH**	70.1	126.1	**M3a**	B3LYP	34.9	36.4	24.3
				G2M-RCC5	47.3	48.9	36.8
				CCSD(T)	41.9	43.5	31.4
TS-M2aM4a	70.5	84.7	**M2a**	B3LYP	16.3	15.1	18.1
				G2M-RCC5	20.1	18.9	21.9
				CCSD(T)	19.1	17.9	20.9
M4a	74.4	93.6	**TS-M2aM3a**	B3LYP	−24.0	−22.9	−25.5
				G2M-RCC5	−30.0	−28.9	−31.5
				CCSD(T)	−30.6	−29.4	−32.1
M5a + H_2O[d]	71.7	126.2	**M4a**	B3LYP	3.6 (3.0)	4.4 (3.4)	−5.3 (−5.9)
				G2M-RCC5	5.0 (4.4)	5.8 (5.2)	−3.9(−4.5)
				CCSD(T)	5.3 (4.7)	6.1 (5.5)	−3.6 (−4.2)
R1a + **OH** + H_2O	66.4	163.7	**M5a** + H_2O	B3LYP	12.7	13.9	2.8
				G2M-RCC5	21.4	22.7	11.5
				CCSD(T)	18.1	19.3	8.1
M1d + H_2O	71.8	124.8		B3LYP	0.0	0.0	0.0
				G2M-RCC5	0.0	0.0	0.0
M2d	73.9	95.6	**M1d** + H_2O	B3LYP	−6.0 (−5.6)	−6.5 (−6.1)	2.2(2.4)
				G2M-RCC5	−6.1 (−5.7)	−6.6 (−6.2)	2.1 (2.5)
TS-M2dM3d	73.2	84.7	**M2d**	B3LYP	15.7	14.5	17.7
				G2M-RCC5	14.6	13.4	16.6
M3d	76.1	87.2	**TS-M2dM3d**	B3LYP	−31.5	−31.2	−31.9
				G2M-RCC5	−38.4	−38.0	−38.7
R2d + **OH**	70.1	126.2	**M3d**	B3LYP	34.7	36.2	24.6
				CCSD(T)[c]	39.9	41.5	29.8
TS-M2dM4d	70.5	85.0	**M2d**	B3LYP	14.8	13.5	16.7
				G2M-RCC5	18.7	17.5	20.6
M4d	74.5	93.7	**TS-M2dM4d**	B3LYP	−26.2	−25.0	−27.6
				G2M-RCC5	−32.0	−30.9	−33.4
M5d + H_2O[d]	71.9	125.9	**M4d**	B3LYP	3.6 (3.1)	4.4 (3.9)	−5.2 (−5.8)
				G2M-RCC5	5.0 (4.5)	5.7 (5.2)	−3.9 (−4.5)
R1d + **OH** + H_2O	66.6	161.8	**M5d** + H_2O	B3LYP	14.1	15.2	4.5
				CCSD(T)[c]	17.1	18.3	7.6
M1c + H_2O	71.9	124.7		B3LYP	0.0	0.0	0.0
				G2M-RCC5	0.0	0.0	0.0
M2c	74.0	95.3	**M1c** + H_2O	B3LYP	−5.7 (−5.3)	−6.1 (−5.7)	2.6 (3.0)
				G2M-RCC5	−6.2 (−5.8)	−6.6 (−6.2)	2.1 (2.5)
TS-M2cM3c	73.0	85.2	**M2c**	B3LYP	14.9	13.7	16.7
				G2M-RCC5	13.9	12.7	15.7
M3c	76.0	86.4	**TS-M2cM3c**	B3LYP	−30.7	−30.5	−30.8
				G2M-RCC5	−37.4	−37.3	−37.7
R2c + **OH**	70.1	126.1	**M3c**	B3LYP	33.6	35.2	23.4
				CCSD(T)[c]	39.7	41.2	29.4
TS-M2cM4c	69.7	87.7	**M2c**	B3LYP	22.8	21.9	24.1
				G2M-RCC5	27.2	26.3	28.6
M4c	73.6	98.1	**TS-M2cM4c**	B3LYP	−22.1	−20.8	−23.9
				G2M-RCC5	−27.1	−25.8	−28.9
M1e + H_2O	71.9	124.1		B3LYP	0.0	0.0	0.0
				G2M-RCC5	0.0	0.0	0.0
M2e	73.9	96.5	**M1e** + H_2O	B3LYP	−5.4 (−5.0)	−5.7 (−5.3)	2.6 (3.0)
				G2M-RCC5	−5.1 (−4.7)	−5.4 (−5.0)	2.8 (3.2)
TS-M2eM3e	73.0	85.0	**M2e**	B3LYP	16.1	14.8	18.3
				G2M-RCC5	14.2	12.9	16.4
M3e	75.9	85.8	**TS-M2eM3e**	B3LYP	−32.7	−32.5	−32.8
				G2M-RCC5	−39.6	−39.4	−39.6
R2e + **OH**	70.0	125.9	**M3e**	B3LYP	33.9	35.5	23.5
				CCSD(T)[c]	39.5	41.1	29.1
TS-M2eM4e	70.4	95.7	**M2e**	B3LYP	30.6	30.4	30.7
				G2M-RCC5	36.2	36.1	36.3
M4e	74.5	100.2	**TS-M2eM4e**	B3LYP	−52.3	−52.0	−53.3
				G2M-RCC5	−58.8	−58.5	−59.9

[a] The ZPE and *S* values were computed at the B3LYP/6-31G(d,p) level of theory. [b] Energy values in parentheses are BSSE corrected. [c] Calculations taking into consideration the CCSD(T)/6-311+G(2df,2p) energies of the radical, OH, and the corresponding carbonyl oxide. [d] Values in parentheses are BSSE corrected with respect to **M4a** and **M4d**, respectively.

TABLE 3: Zero Point Energies (ZPE in kcal mol^{-1}), Entropies (*S* in eu), and G2M-RCC5 Reaction and Activation Energies, Enthalpies, and Free Energies (*E*, *H*, and *G* in kcal mol^{-1}) for the Reaction between Water and M1b, M1f, M1g, and M1h[a]

compound	ZPE	S	relative to	E + ZPE[e]	H_{298}[e]	G_{298}[e]
M1b + H_2O	72.0	124.4		0.0	0.0	0.0
M2b	74.4	94.4	**M1b** + H_2O	−6.2 (−5.8)	−6.7 (−6.3)	2.2 (2.6)
TS-M2bM3b	73.4	86.0	**M2b**	11.7	10.6	13.1
M3b	76.5	86.9	**TS-M2bM3b**	−38.1	−38.0	−38.2
R2b + **OH**[c]	70.2	107.1	**M3b**	39.5	41.2	29.2
TS-M2bM4b	70.4	88.2	**M2b**	20.0	19.3	21.2
M4b	73.8	93.4	**TS-M2bM4b**	−7.0	−6.3	−7.8
M5b + H_2O[d]	71.0	126.6	**M4b**	5.7 (5.2)	6.7 (6.2)	−3.2 (−3.7)
R1b + **OH** + H_2O[c]	67.2	163.8	**M5b** + H_2O	−19.0	−17.7	−28.8
M1f + H_2O	71.8	125.7		0.0	0.0	0.0
M2f	74.1	96.0	**M1f** + H_2O	−5.9 (−5.5)	−6.5 (−6.1)	2.4 (2.8)
TS-M2fM3f	73.6	86.2	**M2f**	9.8	8.6	11.5
M3f	76.5	88.2	**TS-M2fM3f**	−38.9	−38.7	−39.3
R2f + **OH**[c]	70.1	125.2	**M3f**	39.7	41.1	30.0
TS-M2fM4f	70.2	89.0	**M2f**	20.6	19.8	21.9
M4f	73.6	94.0	**TS-M2fM4f**	−7.8	−7.2	−8.6
M5f + H_2O[d]	74.6	126.7	**M4f**	9.0 (8.5)	6.0 (5.5)	−3.7 (−4.3)
R1f + **OH** + H_2O[c]	66.9	164.4	**M5f** + H_2O	−23.0	−17.8	−29.1
M1g + H_2O	72.1	124.1		0.0	0.0	0.0
M2g	74.1	96.6	**M1g** + H_2O	−4.5 (−4.1)	−4.8 (−4.4)	3.5 (3.9)
TS-M2gM3g	73.5	84.9	**M2g**	10.0	8.7	12.1
M3g	76.3	86.8	**TS-M2gM3g**	−36.6	−36.4	36.9
R2g + **OH**[c]	70.1	125.2	**M3g**	38.0	39.4	27.9
TS-M2gM4g	70.4	95.2	**M2g**	37.0	36.8	37.2
M4g	74.5	99.9	**TS-M2gM4g**	−59.4	−59.0	−60.4
M1h + H_2O	72.2	124.1		0.0	0.0	0.0
M2h	74.5	93.8	**M1h** + H_2O	−5.8 (−5.3)	−6.4 (−5.9)	2.7 (3.2)
TS-M2hM3h	73.7	84.9	**M2h**	9.7	8.7	11.4
M3h	76.4	87.2	**TS-M2hM3h**	−37.1	−36.8	−37.5
R2h + **OH**[c]	70.4	127.1	**M3h**	38.7	40.2	28.3
TS-M2hM4h	70.5	85.3	**M2h**	40.0	39.1	41.6
M4h	73.7	94.7	**TS-M2hM4h**	−37.9	−36.7	−39.5

[a] The ZPE and *S* values have been computed at the B3LYP/6-31G(d,p) level of theory except for **TS-M2hM4h** and **M4h**, which have been computed at the higher B3LYP/6-311+G(2d,2p) level of theory. [b] Energy values in parentheses are BSSE corrected. [c] Calculation taking into consideration the CCSD(T)/6-311+G(2df,2p) energies of the radical, OH, and the corresponding carbonyl oxide. [d] Values in parentheses are BSSE corrected with respect to **M4b** and **M4f**, respectively.

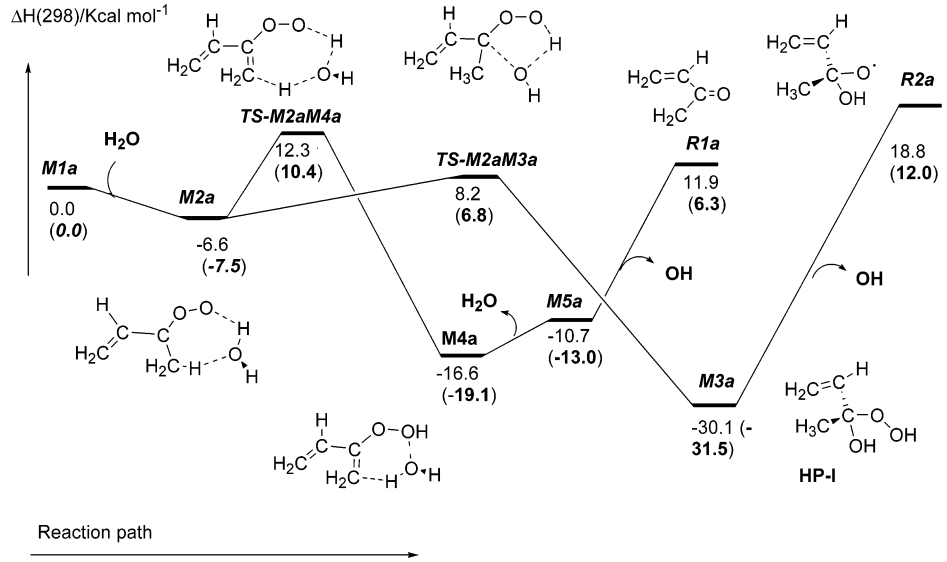

Figure 2. Schematic enthalpy diagram for the reaction between **M1a** and H_2O. The enthalpy values are those computed at the G2M-RCC5 (without parenthesis) and CCSD(T)/6-311+G(2df,2p)//B3LYP/6-311+G(2d,2p) (in parentheses) levels of theory.

energies of a series of compounds. A small absolute average deviation (AAD) of 1.3 kcal mol^{-1} has been obtained between theory and experiment with a largest deviation of 3.3 kcal mol^{-1}.[66]

In the case of the reaction between **M1a** and H_2O, CCSD(T)/6-311+G(2df,2p)//B3LYP/6-311+G(2df,2p) energy calculations have been carried out for all the stationary points. The relative reaction and activation energies have been compared with the G2M-RCC5 and B3LYP values. Single point CCSD(T)/6-311+G(2df,2p) calculations have also been done for all the carbonyl oxides **M1a**−**M1h** and for all the radicals as well.

Finally, rate constants for several elementary reactions of interest have been computed using classical transition-state theory. G2M-RCC5 and CCSD(T) energies as well as B3LYP/6-31G(d,p) partition functions and zero point corrections have been used. The tunneling corrections to the rate constants have

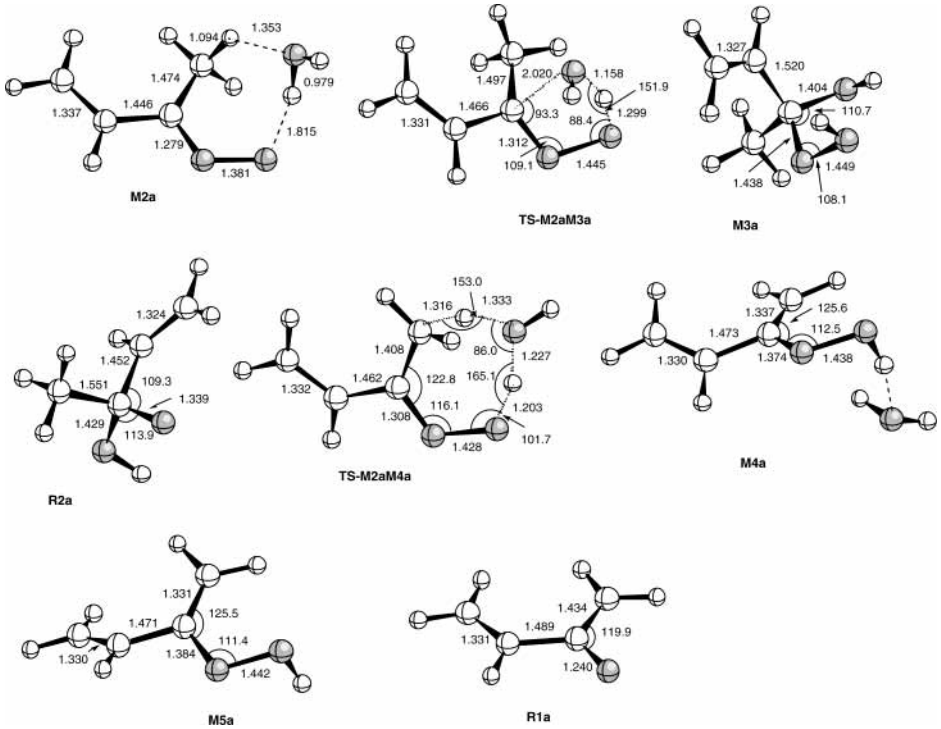

Figure 3. Selected B3LYP/6-311+G(2d,2p) geometrical parameters of the stationary points of the reaction between **M1a** and H_2O.

been considered and computed by the zero-order approximation to the vibrationally adiabatic PES with zero curvature. The unsymmetrical Eckart potential energy barrier approximates the potential energy curve.[69]

All the geometry optimizations and the CCSD(T) calculations have been performed using the Gaussian 94[70] and Gaussian 98[71] suit of programs. The RCCSD(T) calculations over an ROHF wave function for the radicals have been done with the Molcas 4.1[72] program package, and the kinetic results have been obtained with the TheRate program.[73]

Results and Discussion

Along the text, the structures of closed shell minima and radicals are designated by the letters **M** and **R**, respectively, and are followed by a number (**1**, **2**, and so on). As pointed out in eqs 1b and 1c, the different carbonyl oxides are distinguished from each other by adding the letters **a**, **b**, and so on. The same letter is maintained if we consider the reaction of a given carbonyl oxide with water. For example, **M3a** is a minimum from the addition of **M1a** + H_2O, **M3b** corresponds to the equivalent structure from **M1b** + H_2O. The small suffix letters distinguishes isomers of a given compound. The transition states are labeled by **TS** followed by the names of the two connected minima. Thus, for instance, **TS-M2aM3a** corresponds to the transition state connecting **M2a** with **M3a**. In this paper, only relative energies and several selected geometrical parameters are reported. Cartesian coordinates of all the structures and the corresponding absolute energy values are available in the Supporting Information.

The Isoprene Carbonyl Oxides. Results reported very recently by Zhang et al.[40,41] estimate that the reaction between isoprene and ozone is exothermic by about 50 kcal mol^{-1} (eq 1a) and produces nearly equal yields of 1,2-ozonide and 3,4-ozonide (0.59 and 0.41, respectively). Equations 1b and 1c also point out that several carbonyl oxide isomers can be formed during the isoprene ozonolysis. The unimolecular decomposition of the 1,2-ozonide gives H_2COO, **M1a**, **M1c**, **M1d**, and **M1e**. According to Zhang et al.[41] the estimated yields of H_2COO, **M1a**, and **M1c** are 0.21, 0.44, and 0.35, respectively. The fate of the 3,4-ozonide decomposition are H_2COO, **M1b**, **M1f**, **M1g**, and **M1h**. Zhang et al.[41] have also estimated that the yields of H_2COO, **M1b**, and **M1h** are 0.51, 0.44, and 0.05, respectively.

The parent H_2COO carbonyl oxide and its unimolecular and water-assisted decomposition have been widely investigated[42−49,59,60,77] and therefore will not be further considered in the present paper. The more relevant geometrical parameters of the **M1a**−**M1h** conformers are shown in Figure 1, while Table 1 contains the relative energies, enthalpies, and free energies computed at the B3LYP/6-311+G(2d,2p)//B3LYP/6-311+G(2d,2p), CCSD(T)/6-311+G(2df,2p)//B3LYP/6-311+G(2d,2p), and G2M-RCC5 levels of theory. The relative stability of these carbonyl oxides (**M1a**−**M1h**) has been recently discussed on the basis of conjugative, hyperconjugative, H-bonding, and steric interactions,[30,40] and the same arguments are also valid in this point. Our calculated geometrical parameters and relative energies are in good agreement with the results reported by these authors.[30,40]

In the present investigation we are interested in the gas-phase reactivity of the vibrationally stabilized carbonyl oxides with water. Thus, it is worth considering the possible conformational changes between isomers **M1a**−**M1h**, which may occur during the stabilization processes. The interconversion barrier between the syn and anti configurations of the carbonyl oxides must be very high[28] and has not been considered here. However, for each carbonyl oxide, rotation along the C_3–C_4 single bond is possible (see Figure 1 for the numbered carbons) and leads to the cis and trans configurations for the vinyl group with respect to the COO moiety. We have looked therefore for the transition structures that connect a cis compound with its corresponding trans isomer. They are labeled **TS-M1aM1d**, **TS-M1cM1e**, **TS-M1bM1f**, and **TS-M1gM1h**, and connect **M1a** with **M1d**, **M1c** with **M1e**, **M1b** with **M1f**, and **M1g** with **M1h**, respectively. The corresponding enthalpy barriers lie in the range of

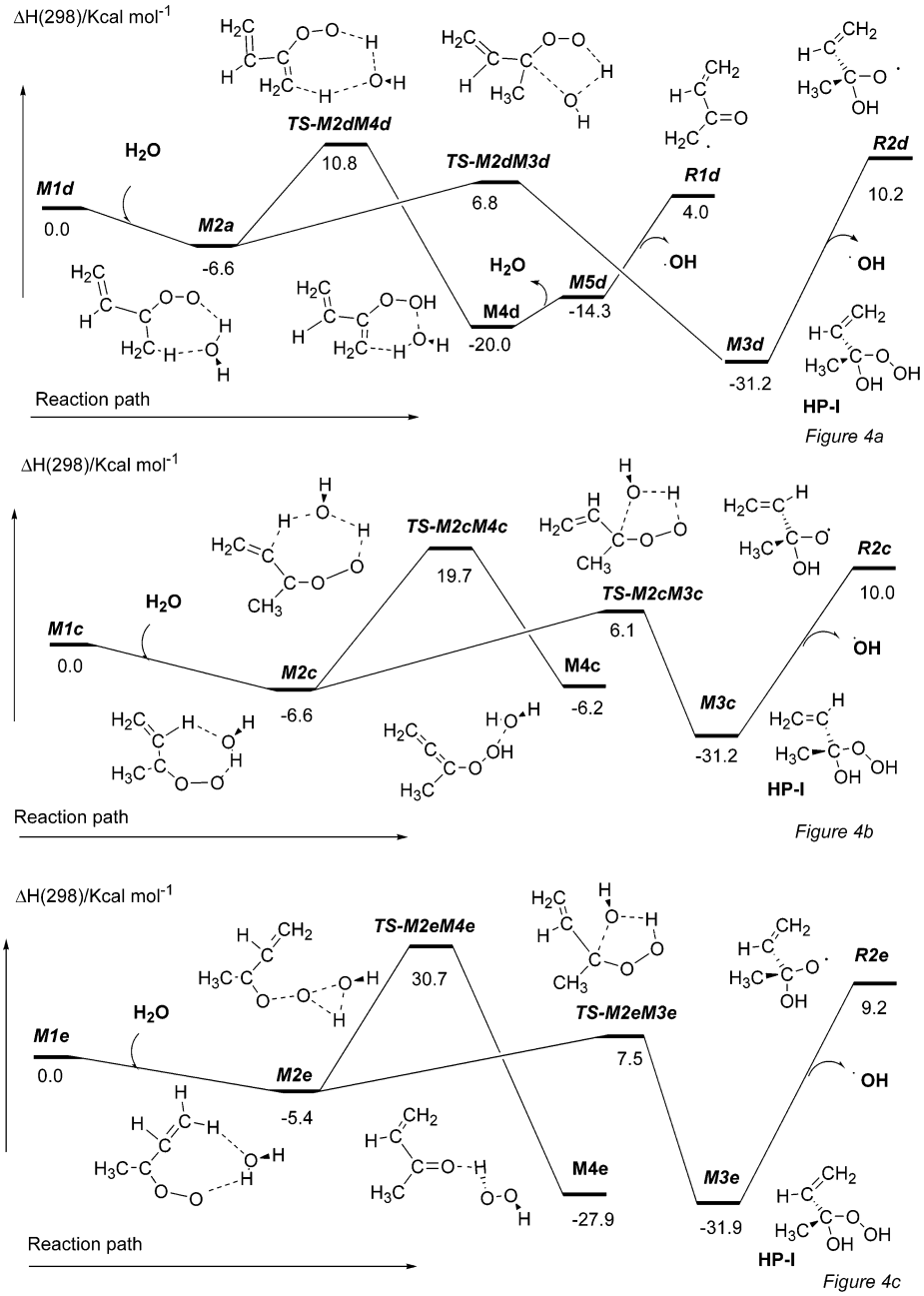

Figure 4. Schematic enthalpy diagram for the reaction of **M1d**, **M1c**, and **M1e** with H_2O. Enthalpies are computed at the G2M-RCC5 level of theory.

7.3−8.6 kcal mol^{-1} at the G2M-RCC5 level (see Table 1). They are smaller than those required for the respective unimolecular decomposition processes.[30,40] Hence, all these conformational changes will occur in the stabilization processes, and therefore, it is expected that the stabilized carbonyl oxides **M1a** and **M1d** would be equally populated. The same conclusion is valid for the remaining pairs: **M1c**−**M1e**, **M1b**−**M1f**, and **M1g**−**M1h**.

Reaction of Isoprene Carbonyl Oxides with H_2O. The reaction between water and the **M1a**−**M1h** carbonyl oxides follows the three-step mechanisms summarized in eq 2.[61] For each carbonyl oxide, this reaction is initiated by the formation of a hydrogen-bond complex (eq 2a). This complex then follows two different reaction modes: (1) addition of water to carbonyl oxide, producing the corresponding α-hydroxy hydroperoxide (eq 2b), and (2) water-assisted hydrogen migration, which could lead to the formation of OH radicals (eq 2c). Reaction mode 1 can be envisaged as a (symmetry allowed) 1,3 dipolar cycloaddition of water to carbonyl oxide, where the oxygen of water is linked to the carbon atom of the carbonyl oxide while an hydrogen atom of water is transferred to the terminal oxygen of the COO unit. In reaction mode 2, the water molecule assists the H migration toward the terminal oxygen of the COO moiety.

For atmospheric purposes, it is convenient to split the discussion into two groups. In the first one, we will consider the reaction between water and the carbonyl oxides formed from the 1,2-ozonide decomposition (**M1a**, **M1d**, **M1c**, and **M1e**, see eq 1b). In the second one, we will take into consideration the reaction between water and the carbonyl oxides formed from the 3,4-ozonide decomposition (**M1b**, **M1f**, **M1g**, and **M1h**; see eq 1c). Tables 2 and 3 contain the corresponding reaction and activation energies, enthalpies, and free energies, while Figures 2, 4, 5, and 7 display the schematic reaction enthalpy profiles for all the processes. In addition we have collected in Figures 3 and 6 the most relevant geometrical parameters of

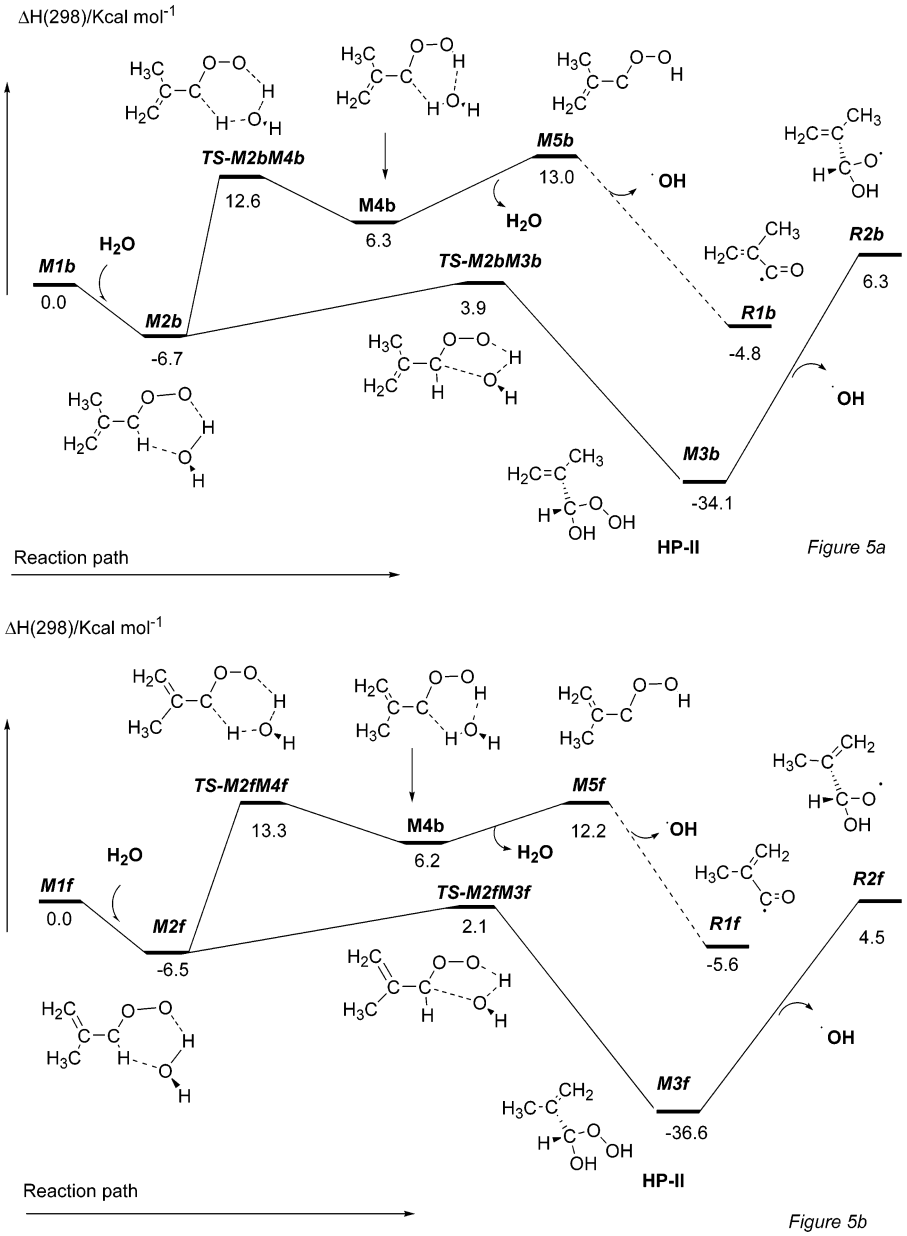

Figure 5. Schematic enthalpy diagram for the reaction of **M1b** and **M1f** with H_2O. Enthalpies are computed at the G2M-RCC5 level of theory.

the compounds involved in the reactions of water with **M1a** and **M1b**, respectively.

(a) Reaction between Water and **M1a**, **M1d**, **M1c**, *and* **M1e** *Carbonyl Oxides.*

Let us first consider the reaction between **M1a** and H_2O. Figure 2 shows that the addition of water to carbonyl oxide first leads to the hydrogen-bond complex **M2a** (reaction mode 1, eq 2a). Then this complex evolves via the transition state **TS-M2aM3a**, to the formation of methylvinyl α-hydroxy hydroperoxide (**M3a**, hereafter labeled as **HP−I**, reaction mode 1 and eq 2b). The corresponding transition structure (see **TS-M2aM3a** in Figure 3) is a five-membered ring where the oxygen of water links the carbon atom (R(CO) = 2.020 Å), while one hydrogen of water is transferred to the terminal oxygen of the COO group (R(OH) = 1.299 Å). At the same time, the peroxide OO bond (R = 1.445 Å) is elongated by 0.081 Å with respect to **M1a** (see Figure 1), thus losing its double bond character.

Furthermore, **M1a** possesses methyl β-hydrogen atoms, which are in syn position with respect to the COO unit. In this case, the process described in eq 2c involves a water-assisted hydrogen migration from the methyl group to the terminal oxygen atom of the COO group. The corresponding seven-membered ring transition structures **TS-M2aM4a** clearly shows the transfer of the hydrogen atom from the methyl group to the water molecule (R(CH) and R(HO) = 1.316 and 1.333 Å, respectively) and the transfer, at the same time, of one hydrogen atom from water to the terminal oxygen of the COO group (R(OH) and R(HO) = 1.227 and 1.203 Å, respectively). Thus, the water molecule acts as a catalyst of the unimolecular hydrogen migration process described in the literature.[30,40,41] The fate of this process is also a hydrogen-bond complex (**M4a**), which is formed between the corresponding hydroperoxide **M5a** and water. Going on along the reaction path, the cleavage of the O−OH bond in **M5** may lead to OH and **R1** radicals (see Figure 2). This reaction mode may therefore be considered as a possible source of atmospheric OH radicals.

Regarding the energetics of the reaction between **M1a** and H_2O, Table 2 shows that electron correlation and basis set effects are important in computing activation and reaction

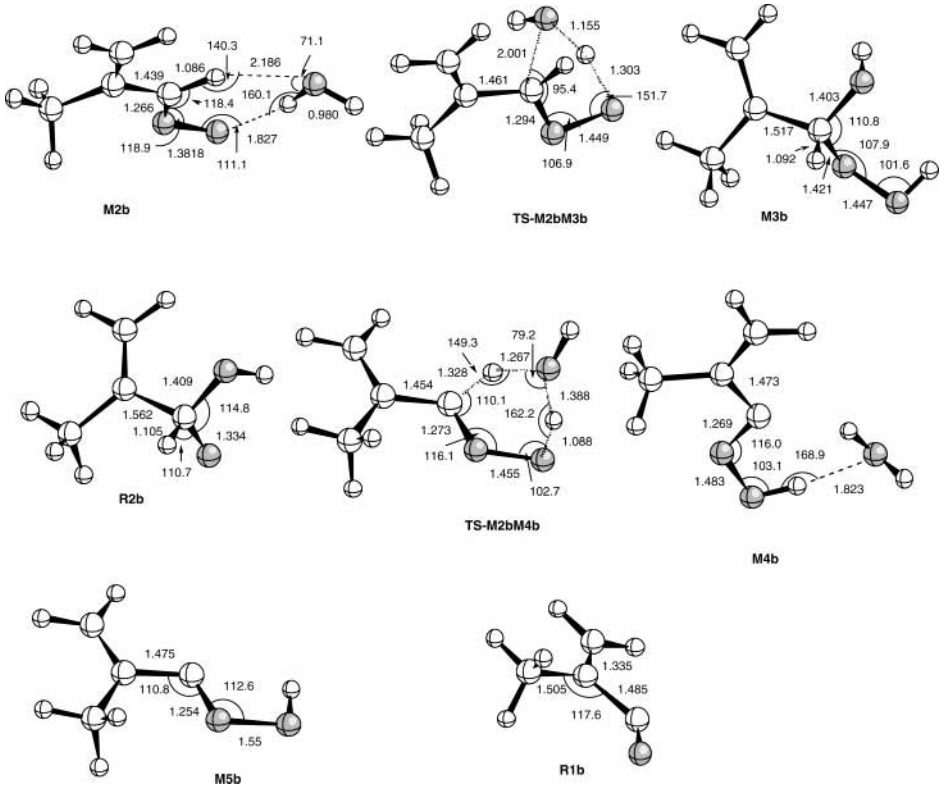

Figure 6. Selected B3LYP/6-311+G(2d,2p) geometrical parameters of the stationary points involved in the reaction between **M1b** and H_2O.

energies. The initial hydrogen-bond complex **M2a** is calculated to be between 6.0 and 7.1 kcal mol^{-1} more stable than the reactants. Furthermore B3LYP/6-311+G(2d,2p)//B3LYP/6-311+G(2d,2p) calculations predict the H migration process (**TS-M2aM4a**) as the most favorable pathway, while the water addition process (**TS-M2aM3a**) leading to the α-hydroxy hydroperoxyde (**HP−I**), requires a higher activation enthalpy (0.8 kcal mol^{-1}). However, more accurate CCSD(T)/6-311+G(2df,2p)//B3LYP/6-311+G(2d,2p) calculations give opposite results, since the activation enthalpy for the water-addition process (**TS-M2aM3a**) is 3.5 kcal mol^{-1} lower than the one associated to the H migration path (**TS-M2aM4a**). Thus, the B3LYP method clearly underestimates the hydrogen-migration barrier. These results are in line with previous studies regarding the poor aggreement of the B3LYP methods for the barrier highs of hydrogen-abstraction reactions.[80−82] This is very important because considering only the B3LYP energies would lead to the *erroneous conclusion* that the most favorable pathway would produce hydroperoxide **M5a**, which could decomposes to OH and **R1a** radicals by O−OH bond breaking. The importance of correlation effects are also pointed out in the relative stability of the products **M3a** and **M4a**, which are computed to be about 7.0 kcal mol^{-1} more stable at the CCSD(T) than at the B3LYP level of theory. These results are in clear accordance with previous theoretical studies on the reaction between water and the parent H_2COO and the methyl- and dimethyl-substituted carbonyl oxides, recently reported in the literature.[60,61]

At this point it is also worth comparing the water-assisted migration process (**TS-M2aM4a**) with the corresponding unimolecular reaction reported by Zhang et al.[40] Although water catalysis reduces the activation enthalpy by about 6 kcal mol^{-1} with respect to the unimolecular decomposition, the water addition path has a lower activation enthalpy and hence is expected to be the most favorable reaction.

As CCSD(T)/6-311+G(2df,2p) single point energy calculations are very time-consuming, less demanding G2M-RCC5 calculations have also been performed. Table 2 shows that relative activation and reaction energies computed at both levels of theory only differ by 0.1−1.0 kcal mol^{-1}, except for the radicals (**R2a** + OH and **R1a** + OH), for whom the energy is underestimated by 3.5 and 5.5 kcal mol^{-1} respectively by the G2M-RCC5 method. Moreover, the relative ordering along the reaction path is the same at the two levels. In view of these results, we will consider G2M-RCC5 energies for the remaining elementary reactions studied, except for all radicals, which will be computed at the CCSD(T)/6-311+G(2df,2p)//B3LYP/6-311+G(2d,2p) level of theory.

Table 2 and Figure 4 show that reactions between water and **M1d**, **M1c**, and **M1e** follow the same trends described above for **M1a** + H_2O. The water addition process (**TS-M2M3**) producing **HP−I** (**M3d**, **M3c**, and **M3e**, respectively) remains the most favorable reaction path. Activation enthalpies are computed to be about 13 kcal mol^{-1} (relative to the **M2** complexes) and the processes are exothermic by about 31 kcal mol^{-1}. The H migration path occurs through **TS-M2M4**. In the case of the reaction between **M2d** and H_2O, the transition structure (**TS-M2dM4d**) is a conformer of the above-discussed **TS-M2aM4a**. As in the case of **M1a**, the two activation barriers of **TS-M2dM3d** and **TS-M2dM4d** are very close. On the other hand, **M1c** and **M1e** possess vinyl H atoms that might migrate to produce 1-methyl-1-hydroperoxyallene (**M4c**) and methyl vinyl ketone (**M4e**), respectively, via the two water-assisted **TS-M2cM4c** and **TS-M2eM4e**. However, these migration processes require higher enthalpy barriers than the water-addition processes (26.3 and 36.1 kcal mol^{-1} respectively; see Table 2 and Figure 4b,c) and would be therefore unlikely.

Another point of interest for atmospheric purposes refers to the possible cleavage of the O−OH bond in **HP−I**, producing OH plus the corresponding **R2** radicals, respectively. Table 2

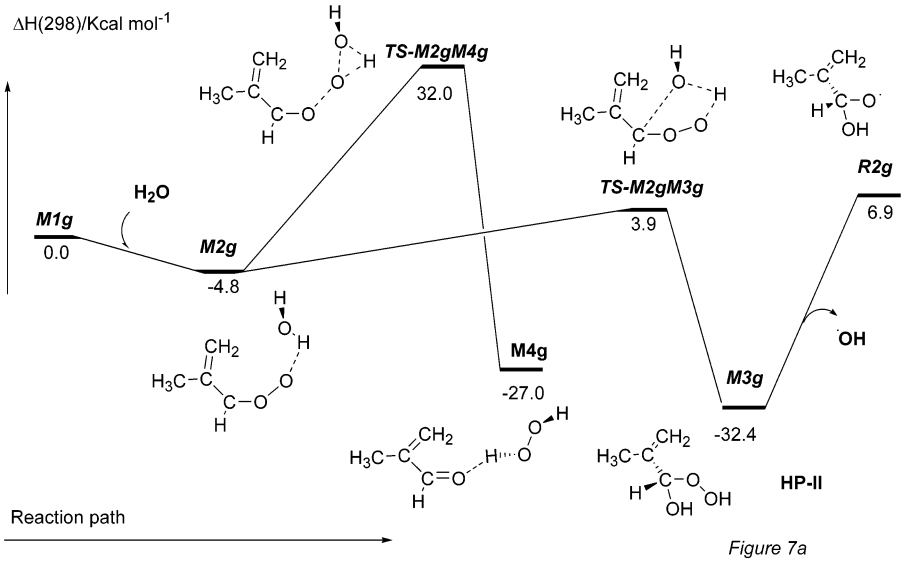

Figure 7a

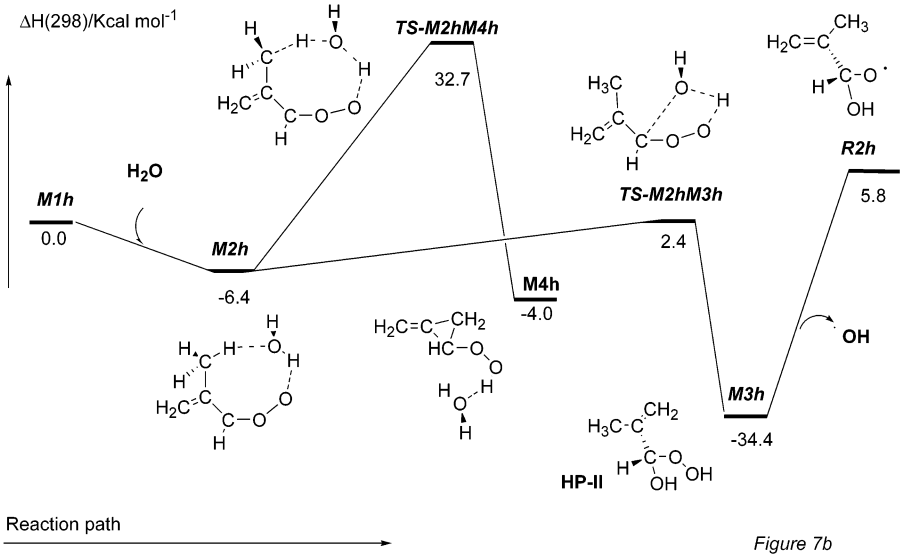

Figure 7b

Figure 7. Schematic enthalpy diagram for the reaction between H_2O and the **M1g** and **M1h** carbonyl oxides, respectively. Enthalpies are computed at the G2M-RCC5 level of theory.

and Figures 2 and 4 display that the α-hydroxy hydroperoxides (**M3a**, **M3d**, **M3c**, and **M3e)** are formed with an excess of energy of about 38 kcal mol^{-1}, whereas the O−OH bond breaking requires a larger energy of about 40−41 kcal mol^{-1}. These results allow us to conclude that this cleavage will not be active under atmospheric conditions and hence, *no additional OH radicals would be formed* via this mechanism.

(b) Reactions between water and **M1b**, **M1f**, **M1g**, and **M1h** Carbonyl Oxides.

Our calculations reveal that the reaction of these species with H_2O follows the same pattern discussed above and schematized in eqs 2. Table 3 and Figures 5 and 7 principally show that (1) the formation of the initial hydrogen-bond complexes (**M2b**, **M2f**, **M2g**, and **M2h**; Figures 5 and 7 and eq 2a) are between 5.5 and 6.3 kcal mol^{-1} more stable than the reactants and (2) the water addition to the carbonyl oxide (via **TS-M2M3**, eq 2b) is the most favorable path. As above, the corresponding transition states for this process are five-membered ring structures (see, for instance **TS-M2bM3b** in Figure 6), in which the oxygen of water links the carbon atom, whereas a hydrogen atom of water is transferred at the same time to the terminal oxygen of the COO moiety. These reactions are exothermic by about 35 kcal mol^{-1} and lead to the formation of different isomers (**M3b**, **M3f**, **M3g**, and **M3h**, respectively) of 2-propenyl α-hydroxy hydroperoxide (hereafter labeled as **HP−II**, eq 2b).

The computed activation enthalpies are in the range of 8.5−10.6 kcal mol^{-1} with respect to corresponding **M2** complex (see Table 3). They are about 4 kcal mol^{-1} smaller than those obtained in the reaction between water and **M1a**, **M1d**, **M1c**, and **M1e** (see above and Table 2). In the case of the carbonyl oxides derived from 1,2-ozonide, the inductive effect of the methyl group linked to the COO group destabilizes the 1,3-cycloaddition with respect to the carbonyl oxides formed from the 3,4-ozonide (**M1b**, **M1f**, **M1g**, and **M1h**), which have a H atom instead of a CH_3 group linked to the COO moiety. A similar effect has been observed in the methyl- and dimethyl-substituted carbonyl oxide recently reported.[61]

The H migration path occurs via **TS-M2M4** (eq 2c) and requires in all cases a larger activation enthalpy than the water addition path (see Table 3).

M1b and **M1f** have one hydrogen atom in the syn position with respect to the COO group, and the corresponding transition state has a six-membered ring structure (see **TS-M2bM4b** in Figure 6) that involves simultaneously the abstraction of the

TABLE 4: Calculated Tunneling Parameters, κ, and Rate Constants, k (s^{-1}), for the Reactions between the Carbonyl Oxides M1a−M1h with H_2O at Different Temperatures[a]

reaction path		273.0 K	280.0 K	290.0 K	298.15 K	300.0 K	310.0 K
				M2a + H_2O			
TS-M2aM3a	κ	1.694	1.618	1.525	1.460	1.446	1.377
		(1.691)	(1.616)	(1.523)	(1.458)	(1.444)	(1.376)
	k_3	0.15275	0.29663	0.72476	1.43670	1.66960	3.64620
		(0.3089)	(0.589)	(1.406)	(2.738)	(3.169)	(6.780)
TS-M2aM4a	κ	123.980	83.441	51.013	36.105	33.586	23.524
		(110.150)	(75.295)	(46.894)	(33.602)	(31.336)	(22.209)
	k_4	1.4478×10^{-2}	2.3912×10^{-2}	4.8834×10^{-2}	8.6922×10^{-2}	9.8983×10^{-2}	1.9828×10^{-1}
		(7.925×10^{-2})	(0.1270)	(0.2486)	(0.4276)	(0.483)	(0.9284)
	$\Gamma = k_4/\kappa$[c]	8.7	7.5	6.3	5.7	5.6	5.2
		(20.4)	(17.7)	(15.0)	(13.5)	(13.2)	(12.0)
				M2d + H_2O			
TS-M2dM3d	κ	1.241	1.204	1.156	1.122	1.114	1.073
	k_3	1.102	2.041	4.671	8.800	10.112	20.823
TS-M2dM4d	κ	91.797	63.733	40.487	29.427	27.525	19.798
	k_4	0.097	0.155	0.302	0.516	0.583	1.110
	$\Gamma = k_4/\kappa$[c,d]	8.11	7.07	6.07	5.54	5.45	5.06
				M2c + H_2O			
TS-M2cM3c	κ	1.430	1.3778	1.312	1.266	1.256	1.206
	k_3	6.942	12.363	26.870	48.674	55.452	109.200
TS-M2cM4c	κ	85.961	58.003	35.887	25.770	24.059	17.204
	k_4	1.9117×10^{-8}	4.4567×10^{-8}	1.4598×10^{-7}	3.7513×10^{-7}	4.6325×10^{-7}	1.4174×10^{-6}
	$\Gamma = k_4/\kappa$[c]	0.00	0.00	0.00	0.00	0.00	0.00
				M2e + H_2O			
TS-M2eM3e	κ	1.285	1.245	1.193	1.156	1.148	1.108
	k_3	1.977	3.581	7.957	14.655	16.756	33.618
TS-M2eM4e	κ	7.403	6.285	5.151	4.486	4.358	3.779
	k_4	6.0272×10^{-16}	2.7690×10^{-15}	2.1998×10^{-14}	1.0903×10^{-13}	1.5515×10^{-13}	9.7853×10^{-13}
	$\Gamma = k_4/\kappa$[c]	0.00	0.00	0.00	0.00	0.00	0.00
				M2b + H_2O			
TS-M2bM3b	κ	1.375	1.328	1.268	1.225	1.216	1.170
	k_3	765.32	1239.4	2369.9	3891.9	4339.4	7639.7
TS-M2bM4b	κ	5.331	4.801	4.194	3.799	3.719	3.340
	k_4	9.5322×10^{-4}	2.1504×10^{-3}	6.4568×10^{-3}	1.5038×10^{-2}	1.8112×10^{-2}	4.7745×10^{-2}
	$\Gamma = k_4/\kappa$[c]	0.00	0.00	0.00	0.00	0.00	0.00
				M2f + H_2O			
TS-M2fM3f	κ	1.044	1.020	b	b	b	b
	k_3	11417.00	17059.00	29579.00	45716.00	50292.00	82521.00
TS-M2fM4f	κ	6.103	5.444	4.695	4.215	4.119	3.664
	k_4	2.9087×10^{-4}	6.6439×10^{-4}	2.0282×10^{-3}	4.7884×10^{-3}	5.7846×10^{-3}	1.5501×10^{-2}
	$\Gamma = k_4/\kappa$[c]	0.00	0.00	0.00	0.00	0.00	0.00
				M2g + H_2O			
TS-M2gM3g	κ	1.107	1.079	1.043	1.016	1.011	b
	k_3	4066.60	6090.60	10477.00	15858.00	17366.00	28341.00
TS-M2gM4g	κ	6.144	5.316	4.452	3.933	3.832	3.368
	k_4	1.3079×10^{-16}	6.3220×10^{-16}	5.3574×10^{-15}	2.7833×10^{-14}	4.0006×10^{-14}	2.6556×10^{-13}
	$\Gamma = k_4/\kappa$[c]	0.00	0.00	0.00	0.00	0.00	0.00
				M2h + H_2O			
TS-M2hM3h	κ	1.087	1.060	1.026	1.001	b	b
	k_3	14812	22217	38302	58079	63935	1.0562×10^5
TS-M2hM4h	κ	1.2838	1.2428	1.1910	1.1537	1.1458	1.1060
	k_4	1.87×10^{-21}	1.14×10^{-20}	1.31×10^{-19}	8.44×10^{-19}	1.27×10^{-18}	1.07×10^{-17}
	$\Gamma = k_4/\kappa$[c]	0.00	0.00	0.00	0.00	0.00	0.00

[a] k_3 and k_4 correspond to the **TS-M2M3** and **TS-M2M4** paths, respectively. The partition functions have been calculated at the B3LYP/6-31G(d,p) level of theory and the energies at the G2M-RCC5 level of theory. The values in parentheses are obtained using energies computed at the CCSD(T)/6-311+G(2df,2p)//B3LYP/6-311+G(2d,2p) level of theory. [b] $\kappa < 1$ and therefore tunneling was not taken into consideration. [c] $\Gamma = k_4/\kappa$ corresponds to the branching ratio (in percent) for the water-catalyzed hydrogen transfer process described by eq 2c. k_4 is the computed rate constant for the corresponding **TS-M2M4** process, while $k = k_3 + k_4$ is the total rate constant. [d] Scaling the branching ratio by 2.3 (see text), we may estimate the following branching ratios at the given temperature: 18.7 (273.0 K), 16.3 (280.0 K), 14.0 (290.0 K), 12.7 (298.15 K), 12.5 (300.0 K), 11.6 (310.0 K).

β-hydrogen atom of the carbonyl oxide by the water molecule (R(CH) and R(HO) = 1.328 and 1.267 Å, respectively) and the transfer of one hydrogen atom from water to the terminal oxygen of the COO group (R(OH) and R(HO) = 1.388 and 1.088 Å, respectively). Table 3 and Figure 5 indicate that the computed activation enthalpies are equal to 19.3 and 19.8 kcal mol^{-1} (relative to **M2b** and **M2f**, respectively). The products are the hydrogen-bond complexes **M4b** and **M4f**, which are formed by the association of corresponding hydroperoxides (**M5b** and **M5f**, respectively) and water. The processes are endothermic by about 13 kcal mol^{-1}. By comparing this water-assisted H migration with the corresponding unimolecular

process reported by Gutbrod et al.[30] and by Zhang et al.,[40] we observe an important catalytic effect of water of about 25 kcal mol^{-1}. However, despite this large catalytic effect, the H migration pathway remains very unlikely in the atmosphere. We may note that a further cleavage of the O−OH bond of **M5b** and **M5f** would give OH plus **R1b** and **R1f** radicals, respectively. Table 3 and Figure 5a,b show that this O−OH bond breaking is exothermic by about 18 kcal mol^{-1}, and a transition state is expected in each case. As quoted before, this pathway will not be active, and therefore, we did not look for each transition state.

In the case of **M1g** and **M1h**, Figure 7 shows that the H migration process would lead to the exothermic formation of **MAC** + H_2O_2 and 2-methylenecyclopropyl hydroperoxide + H_2O, respectively. However, the corresponding activation enthalpies are much higher than those encountered for the addition reaction (36.8 and 39.1 kcal mol^{-1}; Table 3) and make this process unlikely.

Finally, Table 3 and Figures 5 and 7 point out clearly that the cleavage of the O−OH bond in **HP−II** (**M3b**, **M3f**, **M3g**, and **M3h**), which produces OH plus the corresponding **R2** radicals, is endothermic by about 40 kcal mol^{-1}. Thus, for all isomers the required energy is larger than the one released in the formation of the **M3** intermediate. Hence, we can also conclude here that *no additional OH radicals would be formed* via this mechanism.

(c) Kinetic Calculations. To determine the competition between processes 2b and 2c, rate constants of the reactions between all the carbonyl oxides with water have been calculated using the classical transition state theory. Since the reaction is initiated by the formation of a hydrogen-bond complex having a relatively large stability, we have considered the unimolecular processes, which begin at the corresponding **M2** hydrogen-bond complex. A more accurate determination of the rate constant should take into consideration the equilibrium between the reactants and the complex **M2** (eq 2a), which is in part shifted to the reactants because of the entropy change (see Tables 2 and 3). However, this equilibrium should not affect the branching ratio $\Gamma = k_4/k_t$, where k_t is the sum of rate constants $k_4 + k_3$, relative to the reactions through **TS-M2M4** and **TS-M2M3**, respectively. Please note that Γ is the branching ratio of the hydroxyperoxide (**M4**) formed. Due to the fact that important isoprene emissions to the troposphere have been observed in summer and in winter as well, the rate constants in the temperature range of 273.0−310.0 K have been computed. The corresponding data are collected in Table 4.

The branching ratio values of this table show that the hydroperoxide channel is only active for the reaction between water and **M1a** and **M1d**, which have *syn*-methyl hydrogen atoms in β-position with respect to the COO unit. For the remaining carbonyl oxides, α-hydroxy hydroperoxides (**HP−I** and **HP−II**) will be exclusively formed.

The reaction between **M1a** and **M1d** with water differs in a conformational change of the vinyl substitute, and as discussed previously, it is expected that both conformers be equally populated after the stabilization process. For the reaction between **M1a** and H_2O, rate constants and branching ratio have been computed at the two G2M-RCC5 and CCSD(T)/6-311+G(2df,2p)//B3LYP/6-311+G(2d,2p) levels of theory. The more accurate CCSD(T) calculations predict activation barriers 1.0 and 0.4 kcal mol^{-1} smaller than those obtained at the G2M-RCC5 level for **TS-M2aM4a** and **TS-M2aM3a**, respectively (see Table 2). These small energy differences naturally yield to larger differences for the computed rate constants and consequently for the prediction of the branching ratio. Thus, the production of **M4a** is predicted to be 2.3 times larger using the more accurate CCSD(T)/6-311+G(2df,2p)//B3LYP/6-311+G(2d,2p) energies than the G2M-RCC5 energies (see Table 4). This factor is more or less maintained along the temperature range considered. A very interesting and unexpected result from Table 4 refers to the Γ branching ratio along the temperatures considered. Our calculations indicate that Γ increases as T decreases, with values of 12% at 310 K, 15% at 290%, and up to 20.4% at 273 K (see Table 4). This unexpected effect is due to the quantum mechanical tunneling correction factor κ for **TS-M2aM4a**, which is computed to be 22.2 at 310 K and rises at lower temperatures up 110.15 at 273 K.

For the reaction between **M1d** and H_2O, the rate constants and branching ratios have been computed only at the G2M-RCC5 level. The theoretical values are very similar to those obtained for the **M1a** + H_2O reaction at the same level (both reactions describe the same process and differ in rotational change of the vinyl substitute). Therefore, we may consider the same scaling factor of 2.3 and estimate the OH production ratio from 11.6% at 310 K to about 19% at 273 K (see footnote *d* in Table 4).

Here, it is worth pointing out that formation of **M5a** and **M5d** could be associated with the formation of OH radicals through the cleavage of the O−OH bond, although these hydroperoxides could be also collisionally stabilized (see Figures 2 and 4a and Table 2). This point requires further work to be clarified. However, the features of this reaction and the competition with the formation of **HP−I** should be easily distinguished experimentally. According to the reaction mechanism displayed in Figures 2 and 4a, and doing experiments with D_2O instead of H_2O, the vinyl hydroperoxides **M5a** and **M5d** will be deuterated and the hydroxyl radical, if produced, should be also deuterated. Moreover, and taking into consideration that water acts as a catalyst of this process, we should obtain DHO in any case.

Conclusions

The theoretical investigation presented in this paper reveals several important aspects regarding the gas phase reactivity of the vibrationally stabilized isoprene carbonyl oxides with water, which has importance in atmospheric chemistry.

(1) The reaction between water and carbonyl oxide begins with the formation of a hydrogen-bond complex (eq 2a), which is about 6 kcal mol^{-1} more stable than the reactants. Then the reaction can follow two reaction modes: (a) water addition to carbonyl oxide (eq 2b), which produces α-hydroxy hydroperoxyde, and (b) water-assisted hydrogen migration to the terminal oxygen of the COO group (eq 2c). The water addition is the most favorable reaction mode with activation enthalpies of about 14 kcal mol^{-1} (relative to the initial H-bond complex) for carbonyl oxides derived from the 1,2-ozonide and about 9 kcal mol^{-1} for carbonyl oxides derived from the 3,4-ozonide. The water-assisted hydrogen migration path corresponds to the water-catalyzed reaction of the unimolecular decomposition path reported in the literature, which is responsible for the OH radical production in the isoprene ozonolysis.[30,40] Although the water catalytic effect is important (between 6 and 25 kcal mol^{-1}), the resulting activation barriers are higher than those encountered for the water addition reaction mode.

(2) There are noticeable differences in the calculated reaction and activation enthalpies between the B3LYP/6-311+G(2d,2p)//B3LYP/6-311+G(2d,2p) method on one hand and the CCSD(T)/6-311+G(2df,2p)//B3LYP/6-311+G(2d,2p) and the G2M-RC5 methods on the other hand. The B3LYP

approach performs well for the hydrogen-bond complexes but underestimates the hydrogen transfer barriers significantly. This may lead to erroneous conclusions on the product distributions. G2M-RCC5 performs quite well except for the radicals, for whose the energies are significantly underestimated

(3) Since isoprene emission have been observed in winter and summer as well, the rate constants relative to the reactions between carbonyl oxides with water and the branching rations in the 273−310 K range have been computed. Only for the reaction of water with **M1a** and **M1d** (which have β-hydrogen atoms in syn position with respect to the COO unit) is the hydrogen transfer reaction mode active (eq 2b). This reaction could produce *OH radicals* or a collisionally stabilized vinyl hydroperoxide. In that case, the branching ratio for the hydrogen transfer reaction is computed to be about 13% at 298.15 K, but rises up to 20% at 273 K due to an important tunneling effect. For the remaining carbonyl oxides, only the formation of α-hydroxy hydroperoxydes is active. Experiments with D_2O are proposed, which will easily check the reliability of this mechanism.

Acknowledgment. The financial support for this work was provided by the Dirección General de Investigación Científica y Técnica (DGICYT, Grant BQU2002-0485-C02-01) and by the Generalitat de Catalunya (Grant 2001SGR00048). P.A. thanks the European Community—Access to Research Infrastructure Action of the Improving Human Potential Program—for financial support. The calculations described in this work were performed at the Centre de Supercomputació de Catalunya (CESCA), whose services are gratefully acknowledged. The comments and suggestions of the anonymous referees are also acknowledged.

Supporting Information Available: The Cartesian coordinates and absolute energies of all stationary points reported in this paper. This material is available free of charge via the Internet at http://pubs.acs.org.

References and Notes

(1) Chameides, W. L.; Lindsay, R. W.; Richardson, J.; Kiang, C. S. *Science* **1988**, *241*, 1473.
(2) Trainer, M.; Williams, E.; Parrish, D.; Burhr, M.; Allwine, E.; Westberg, H.; Fehsenfeld, F.; Liu, S. *Nature* **1987**, *329*, 705.
(3) He, C.; Murray, F.; Lyons, T. *Atmos. Environ.* **2000**, *34*, 64
(4) Wayne, R. P. *Chemistry of Atmospheres*; Oxford University Press: New York, 2000.
(5) Carslaw, N.; Bell, N.; Lewis, A. C.; McQuaid, J. B.; Pilling, M. J. *Atmos. Environ.* **2000**, *34*, 2827.
(6) Shallcross, D. E.; Monks, P. S. *Atmos. Environ.* **2000**, *34*, 1659.
(7) Kesselmeier, J.; Bode, K.; Torres, L. *Atmos. Environ.* **1998**, *32*, 1947.
(8) Kesselmeier, J.; Schafer, L.; Torres, L. *Atmos. Environ.* **1996**, *30*, 1841.
(9) Lamb, B.; Guenther, A. B.; Gay, D.; Westberg, H. *Atmos. Environ.* **1987**, *21*, 1695.
(10) Guenther, A. B.; Zimmerman, P. R.; Harley, P. C. *J. Geophys. Res.* **1993**, *99*, 12609.
(11) Reimann, S.; Calanca, P.; Hofer, P. *Atmos. Environ.* **2000**, *34*, 109. Heeb, N. V.; Forss, A.-F.; Bach, C. *Atmos. Environ.* **1999**, *33*, 205.
(12) Atkinson, R. *J. Phys. Chem. Ref. Data* **1994**, *Monograph 2*, 1.
(13) Atkinson, R.; Aschmann, S. M.; Arey, J.; Shorees, B. *J. Geophys. Res.* **1992**, *97*, 6065.
(14) Atkinson, R.; Aschmann, S. M. *Environ. Sci. Technol.* **1993**, *27*, 1357.
(15) Atkinson, R.; Tuazon, E. C.; Aschmann, S. M. *Environ. Sci. Technol.* **1995**, *29*, 1860.
(16) Paulson, S. E.; Orlando, J. J. *Geophys. Res. Lett.* **1996**, *23*, 3727.
(17) Paulson, S. E.; Sen, A. D.; Liu, P.; Fenske, J. D.; Fox, M. J. *Geophys. Res. Lett.* **1997**, *24*, 3193.
(18) Pfeiffer, T.; Forberich, O.; Comes, F. J. *Chem. Phys. Lett.* **1998**, *298*, 3251.
(19) Donahue, N.; Kroll, J. H.; Anderson, J. G. *Geophys. Res. Lett.* **1998**, *25*, 59.
(20) Paulson, S. E.; Chung, M. Y.; Hasson, A. S. *J. Phys. Chem. A* **1999**, *103*, 8127.
(21) Paulson, S. E.; Fenske, J. D.; Sen, A. D.; Callahan, T. W. *J. Phys. Chem. A* **1999**, *103*, 2050.
(22) Neeb, P.; Moortgat, G. K. *J. Phys. Chem. A* **1999**, *103*, 9003.
(23) Mihelcic, D.; Heitlinger, M.; Kley, D.; Müsgen, P.; Volz-Thomas, A. *Chem. Phys. Lett.* **1999**, *301*, 559.
(24) (a) Lewin, A. G.; Johnson, D.; Price, D. W.; Marston, G. *Phys. Chem. Chem. Phys.* **2001**, *3*, 1253. (b) Johnson, D. Lewin, A. G.; Martson, G. *J. Phys. Chem. A.* **2001**, *105*, 2933. (c) Rickard, A. R.; Johnson, D.; McGill, C. D.; Martson, G. *J. Phys. Chem. A.* **1999**, *103*, 7656.
(25) Kroll, J. H.; Clarke, J. S.; Donahue, N. M.; Anderson, J. G.; Demerjian, K. L. *J. Phys. Chem. A* **2001**, *105*, 1554.
(26) Kroll, J. H.; Clarke, J. S.; Donahue, N. M.; Anderson, J. G.; Demerjian, K. L. *J. Phys. Chem. A* **2001**, *105*, 4446.
(27) Paulson, S. E.; Flagan, R. C.; Seinfeld, J. H. *Int. J. Chem. Kinet.* **1992**, *24*, 103.
(28) Anglada, J. M.; Bofill, J. M.; Olivella, S.; Solé, A. *J. Am. Chem. Soc.* **1996**, *118*, 4636.
(29) Gutbrod, R.; Schindler, R. N.; Kraka, E.; Cremer, D. *Chem. Phys. Lett.* **1996**, *252*, 221.
(30) Gutbrod, R.; Kraka, E.; Schindler, R. N.; Cremer, D. *J. Am. Chem. Soc.* **1997**, *119*, 7330.
(31) Olzmann, M.; Kraka, E.; Cremer, D.; Gutbrod, R.; Andersson, S. *J. Phys. Chem.* **1997**, *101*, 9421.
(32) Cremer, D.; Kraka, E.; Sosa, C. *Chem. Phys. Lett.* **2001**, *337*, 199.
(33) Sander, W.; Block, K.; Kappert, W.; Kirschfeld, A.; Muthusamy, S.; Schroeder, K.; Sosa, C. P.; Kraka, E.; Cremer, D. *J. Am. Chem. Soc.* **2001**, *123*, 2618.
(34) Calvert, J. G.; Lazrus, A.; Kok, G. L.; Heikes, B. G.; Walega, J. G.; Lind, J.; Cantrell, C. A. *Nature* **1985**, *317*, 27.
(35) Möller, D. *Atmos. Environ.* **1989**, *23*, 1625.
(36) Hewitt, C. N.; Kok, G. L.; Fall, R. *Nature* **1990**, *344*, 56.
(37) Criegee, R. *Angew. Chem., Int. Ed. Engl.* **1975**, *14*, 745.
(38) Anglada, J. M.; Crehuet, R.; Bofill, J. M. *Chem. Eur. J.* **1999**, *5*, 1809.
(39) Fenske, J. D.; Hasson, A. L.; Paulson, S. E.; Kuwata, K. T.; Ho, A.; Houk, K. N. *J. Phys. Chem. A* **2000**, *104*, 7821.
(40) Zhang, D.; Zhang, R. *J. Am. Chem. Soc.* **2002**, *124*, 2692.
(41) Zhang, D.; Zhang, R. *Chem. Phys. Lett.* **2002**, *358*, 171.
(42) Neeb, P.; Horie, O.; Moortgat, G. K. *J. Phys. Chem. A* **1998**, *102*, 6778.
(43) Herron, J. T.; Huie, E. *J. Am. Chem. Soc.* **1977**, *99*, 5430.
(44) Niki, H.; Maker, P. D.; Savage, C. M.; Breitenbach, L. P.; Hurley, M. D. *J. Phys. Chem.* **1987**, *91*, 941.
(45) Martinez, R. I.; Herron, J. T. *J. Phys. Chem.* **1988**, *92*, 4644.
(46) Gutbrod, R.; Kraka, E.; Schindler, R. N.; Cremer, D. *J. Am. Chem. Soc.* **1997**, *119*, 7330.
(47) Anglada, J. M.; Bofill, J. M.; Olivella, S.; Solé, A. *J. Phys. Chem. A* **1998**, *19*, 3398.
(48) Chen, B. Z.; Anglada, J. M.; Huang, M. B.; Kong, F. *J. Phys. Chem. A* **2002**, *106*, 1877.
(49) Paulson, S. E.; Chung, M. Y.; Hasson, A. S. *J. Phys. Chem. A* **1999**, *103*, 8127.
(50) Becker, K. H.; Barnes, I.; Ruppert, L.; Wiesen, P. *Free Radicals in Biology and Environment*; F. Minisci Edition, Kluwer Academic Publishers: Dordretch, 1996; p 365.
(51) Jenkin, M. E.; Saunders: S. M.; Pilling, M. J. *Atmos. Environ.* **1997**, *31*, 81.
(52) Puxbaum, H.; Rosenberg, C.; Gregori, M.; Lanzerstorfer, C.; Ober, E.; Winiwarter, W. *Atmos. Environ.* **1988**, *22*, 1841.
(53) Hellpointner, E.; Gäb, S. *Nature* **1989**, *107*, 631.
(54) Grosjean, D. *Environ. Sci. Technol.* **1989**, *23*, 1506.
(55) Hewitt, C. N.; Kok, G. L. *J. Atmos. Chem.* **1991**, *12*, 181.
(56) Sanhueza, E.; Santana, M.; Hermoso, M. *Atmos. Environ.* **1992**, *26A*, 1421.
(57) Lawrence, J. E.; Koutrakis, P. *Environ. Sci. Technol.* **1994**, *28*, 957.
(58) Granby, K.; Christensen, C. S.; Lohse, C. *Atmos. Environ.* **1997**, *31*, 1403.
(59) Aplincourt, P.; Ruiz-López, M. F. *J. Am. Chem. Soc.* **2000**, *122*, 8990.
(60) Crehuet, R.; Anglada, J. M.; Bofill, J. M. *Chem. Eur. J.* **2001**, *7*, 2227.
(61) Anglada, J. M.; Aplincourt, P.; Bofill, J. M.; Cremer, D. *ChemPhysChem* **2002**, *2*, 215.
(62) Becke, A. D. *J. Chem. Phys.* **1993**, *98*, 5648.
(63) Hariharan, P. C.; Pople, J. A. *Theor. Chim. Acta* **1973**, *28*, 213.
(64) Krishnan, R.; Binkley, J. S.; Seeger, R.; Pople, J. A. *J. Chem. Phys.* **1980**, *72*, 650.
(65) Boys, S. F.; Bernardi, F. *Mol. Phys.* **1970**, *19*, 553.

(66) Mebel, A. M.; Morokuma, K.; Lin, M. C. *J. Chem. Phys.* **1995**, *103*, 7414.

(67) Cizek, J. *Adv. Chem. Phys.* **1969**, *14*, 35. Barlett, R. J. *J. Phys. Chem.* **1989**, *93*, 1963. Raghavachari, K.; Trucks, G. W.; Pople, J. A.; Head-Gordon, M. *Chem. Phys. Lett.* **1989**, *157*, 479.

(68) Møller, C.; Plesset, M. S. *Phys. Rev.* **1934**, *46*, 618. Pople, J. A.; Binkley, J. S.; Seeger, R. *Int. J. Quantum Chem. Symp.* **1980**, *10*, 1. Krishnan, R.; Pople, J. A. *Int. J. Quantum Chem.* **1978**, *14*, 91. Krishnan, R.; Frisch, M. J.; Pople, J. A. *J. Chem. Phys.* **1980**, *72*, 4244.

(69) Truong, T. N.; Truhlar, D. G. *J. Chem. Phys.* **1990**, *93*, 1761.

(70) Frisch, M. J.; Trucks, G. W.; Schlegel, H. B.; Gill, P. M. W.; Johnson, B. G.; Robb, M. A.; Cheeseman, J. R.; Keith, T.; Petersson, G. A.; Montgomery, J. A.; Raghavachari, K.; Al-Laham, M. A.; Zakrzewski, V. G.; Ortiz, J. V.; Foresman, J. B.; Peng, C. Y.; Ayala, P. Y.; Chen, W.; Wong, M. W.; Andres, J. L.; Replogle, E. S.; Gomperts, R.; Martin, R. L.; Fox, D. J.; Binkley, J. S.; Defrees, D. J.; Baker, J.; Stewart, J. P.; Head-Gordon, M.; Gonzalez, C.; Pople, J. A. *Gaussian 94*, Revision B.3; Gaussian Inc.: Pittsburgh, PA, 1995.

(71) Frisch, M. J.; Trucks, G. W.; Schlegel, H. B.; Scuseria, G. E.; Robb, M. A.; Cheeseman, J. R.; Zakrzewski, V. G.; Montgomery, J. A.; Stratmann, R. E.; Burant, J. C.; Dapprich, S.; Millam, J. M.; Daniels, A. D.; Kudin, K. N.; Strain, M. C.; Farkas, O.; Tomasi, J.; Barone, V.; Cossi, M.; Cammi, R.; Mennucci, B.; Pomelli, C.; Adamo, C.; Clifford, S.; Ochterski, J.; Petersson, G. A.; Ayala, P. Y.; Cui, Q.; Morokuma, K.; Malick, D. K.; Rabuck, A. D.; Raghavachari, K.; Foresman, J. B.; Cioslowski, J.; Ortiz, J. V.; Stefanov, B. B.; Liu, G.; Liashenko, A.; Piskorz, P.; Komaromi, I.; Gomperts, R.; Martin, R. L.; Fox, D. J.; Keith, T.; Al-Laham, M. A.; Peng, C. Y.; Nanayakkara, A.; Gonzalez, C.; Challacombe, M.; Gill, P. M. W.; Johnson, B. G.; Chen, W.; Wong, M. W.; Andres, J. L.; Head-Gordon, M.; Replogle, E. S.; Pople, J. A. *Gaussian 98*, Revision A.5; Gaussian, Inc.: Pittsburgh, PA, 1998.

(72) Andersson, K.; Blomberg, M. R. A.; Fülscher, M. P.; Karlstrom, G.; Lindh, R.; Malmqvist, P.; Neogrady, P.; Olsen, J.; Roos, B. O.; Sadlej, A. J.; Schutz, M.; Seijo, L.; Serrano-Andres, L.; Siegbahn, P. E. M.; Widmark, P. O. *MOLCAS*, Version 4.1; Lund University: Sweden, 1998.

(73) Duncan, W. T.; Truong, T. N. http://therate.hec.utah.edu (accessed September 2000).

(74) Becker, K. H.; Brockmann, K. J.; Bechara, J. *Nature* **1990**, *346*, 256.

(75) Becker, K. H.; Bechara, J.; Brockmann, K. J. *Atmos. Environ.* **1993**, *27A*, 57.

(76) Simonaitis, R.; Olsyna, K. J.; Meagher, J. F. *Geophys. Res. Lett.* **1991**, *18*, 9.

(77) Neeb, P.; Sauer, F.; Horie, O.; Moortgat, G. K. *Atmos. Environ.* **1997**, *31*, 1417.

(78) Sauer, F.; Schäfer, C.; Neeb, P.; Horie, O.; Moortgat, G. K. *Atmos. Environ.* **1999**, *33*, 229.

(79) Kroll. J. H.; Hanisco, T. F.; Donahue, N. M.; Demerjian, K. L.; Anderson, J. G. *Geophys. Res. Lett.* **2001**, *28*, 3863.

(80) Hamprecht, F. A.; Cohen, A. J.; Tozer, D. J.; Handy, N. C. *J. Chem. Phys*. **1998**, *109*, 6264.

(81) Tozer, D. J.; Handy, N. C. *J. Phys. Chem. A* **1998**, *102*, 3162.

(82) Sodupe, M.; Bertran, J.; Rodríguez-Santiago, L.; Baerends, E. J. *J. Phys. Chem. A*, **1999**, *103*, 166.

(83) Aplincourt, P.; Anglada, J. M. *J. Phys. Chem. A* **2003**, *107*, 5812. (following paper in this issue).